Proceedings World Geothermal Congress 2026
Calgary, Canada, June 8 – 11, 2026

Closed-Loop Geothermal Water Quality Management: Can Solid Particles Make It 5 km To Surface?

Kaitlin Foley[1]*, Derek Stephen[1], Mo Abouelhassan[1] and Colin Brown[1]
Eavor Technologies Inc., Calgary, Alberta[1]
kaitlin.foley@eavor.com

Keywords: Geothermal, closed-loop geothermal, advanced geothermal systems, water quality, particle settling, particle size distribution

ABSTRACT

This study investigates the probability of solid particles reaching the surface facilities for a closed-loop geothermal system due to the risk of particle accumulation in the surface equipment. A major concern for facility operation is solids reaching critical surface equipment such as the heat exchangers. This could potentially result in plugging, fouling, and corrosion of the surface equipment. The effects of particle accumulation include reduced fluid flow, an increase in pressure drop, reduced heat transfer efficiency, and structural damage to equipment. Left-over drilling debris has the potential to enter and circulate through the geothermal system's subsurface open hole laterals. The concentration of solids expected during loop circulation start-up and normal operation thereafter is dependent on the initial handover state of the loop from drilling to operations. Once the geothermal working fluid is circulating, flow rate and temperature impact the potential for solids to travel approximately 5 km to surface. Prior to start-up and circulation of the geothermal loop, several calculation methods are employed to estimate the particle distribution at surface. This preliminary analysis is then compared to actual performance data obtained during circulation of the loop working fluid. During drilling activities involving loop circulation, sampling of the geothermal working fluid is performed to provide actual results for particle size distribution. A comparative assessment of the predictive modelling against collected particle data is conducted to inform and refine the accuracy of initial modelling used to predict particles reaching the surface facilities.

1 INTRODUCTION

A major concern for the operation of geothermal facilities is the introduction of unwanted solids into the surface equipment such as power plant components and heat exchangers. These solids are often generated during drilling activities, where agitation and mechanical disturbance of the formation cause fine particles and rock fragments to be mobilized. Solids can also be introduced from fluids used during drilling activities. In geothermal wells that are not fully cased and cemented, the circulating working fluid remains in direct contact with the surrounding rock formation, creating pathways for these particles to enter the fluid stream. As the fluid is brought to the surface, the suspended solids are transported into the surface equipment, where they can have significant effects on operation and production.

The presence of suspended and entrained solids in geothermal fluids can accelerate erosion of pipes, valves, and power plant components, leading to premature material loss and equipment failure. Particle depositions within heat exchangers and piping results in plugging and fouling, reducing flow capacity and thermal efficiency. Over time, these mechanisms collectively contribute to reduced heat transfer performance, increased pressure drops across system components, and the potential for structural damage or unplanned outages. Effective control and removal of solids are therefore critical to maintaining stable operation, minimizing maintenance requirements, and ensuring the long-term reliability of geothermal systems.

Predicting the occurrence and transport behaviour of these solids is inherently challenging due to the depth and complexity of closed-loop geothermal wells. Subsurface conditions are highly variable, and the degree of solids concentrated within the wellbore is often uncertain. Fluid properties and flow rates play a critical role in determining whether particles remain suspended in the working fluid and can be lifted to surface or settle within the bottom of the well. Predictive modelling is therefore an essential tool, providing insights into particle behaviour that support the operational mitigation strategies at the surface to reduce the risk of solid accumulation and subsequent equipment damage.

Governing models such as Stokes' Law provide theoretical guidance on the particle sizes that can be transported to the surface under idealized conditions. However, unknown parameters that cause non-ideal behaviour are difficult to observe. As a result, accurately defining the size distribution of solids downhole is challenging without direct data. Probabilistic modelling can be employed to approximate particle transport behaviour as a size distribution. The acquisition of reliable field data is critical to improve and validate these models, ultimately enhancing their accuracy and effectiveness in reducing risks during closed-loop geothermal operations.

2 SYSTEM DESCRIPTION

2.1 System geometry

Closed-loop geothermal systems, or advanced geothermal systems (AGS), circulate a working fluid through a sealed wellbore to extract heat from the subsurface without direct interaction between the fluid and rock (White et al., 2024). In this study, the system consists of two cased vertical wells connected by multiple open hole horizontal lateral wells forming a subsurface heat exchanger. Lateral wells are sealed with a chemical solution to reduce rock permeability. The working fluid circulates through the loop, absorbs heat via conduction, and returns to the surface through the outlet well to deliver thermal energy before recirculation.

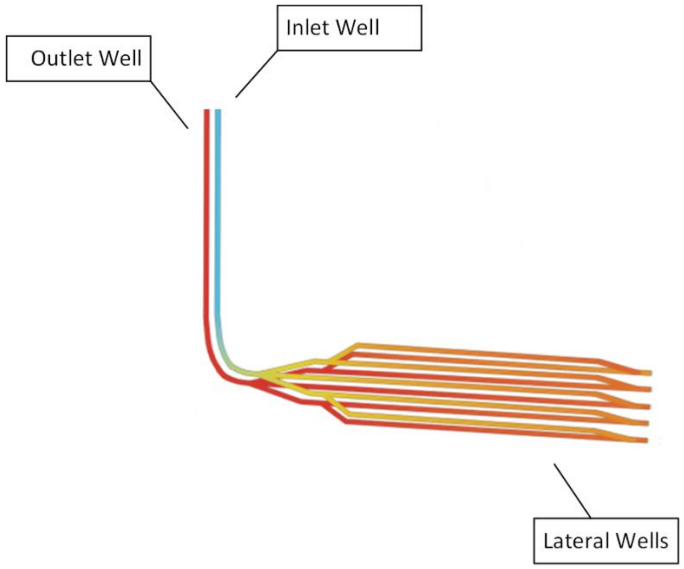


Figure 1. Illustration of a closed-loop geothermal system.

2.2 Fluid composition

The working fluid circulating through the closed-loop system is primarily potable water and initially considered to be homogenous. However, solid particles can be introduced to the fluid from drilling activities and the subsurface rock formation. These sources include:

- Drilling debris: During drilling, agitation of the rock surface loosens rock debris that may accumulate in the lateral wells. While most debris is displaced prior to start-up, some debris may remain downhole.
- Drilling mud: Residual drilling fluids may be forced into the rock formation during drilling. During loop circulation, some drilling fluids may return to the working fluid.

Working fluid entering the loop via the inlet well is assumed to be uncontaminated as it travels approximately 4,500 m downwards through the cased vertical well. Solid debris may be picked up as the working fluid flows through each lateral well. This working fluid then flows back up approximately 4,500 m through the outlet well.

2.3 System assessment

Particle settling models are applied to assess and mitigate solids-related risks to geothermal surface facilities. In this study, several predictive models are evaluated using solids data collected during induced circulation of the closed-loop system prior to start-up. Samples collected at defined flow rates from the outlet wellhead are used to characterize particle settling distributions. Based on the measured solids data and corresponding flow conditions, particle distributions at various operating flow rates can be more accurately estimated.

3 ANALYTICAL MODEL

3.1 Stokes' Law

Stokes' Law is widely applicable in real-world systems, such as those found in oil and gas and geothermal industries, where particle settling plays a critical role in filtration and fluid transport processes. These systems rarely contain particles of a single, uniform size, which makes Stokes' Law a useful analytical model. Stokes' Law provides a deterministic, physics-based solution that relates particle size, density, and fluid viscosity to settling velocity.

Stokes' Law is a principle in fluid mechanics that can be applied to determine the terminal velocity of a small, smooth, spherical particle in a column of fluid under laminar flow conditions. A free body diagram is shown in Figure 2 to illustrate the three main forces acting on a small sphere moving through a viscous fluid.

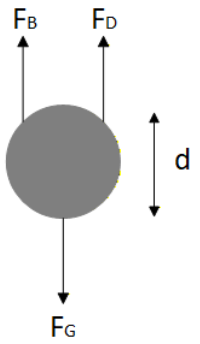


Figure 2. Free body diagram to show forces acting on a spherical particle moving through a viscous fluid.

Terminal velocity is a constant velocity reached when gravitational and buoyant forces balance viscous drag forces. The law states that the force preventing a spherical particle from moving through a viscous fluid is directly proportional to the velocity, radius of the sphere, and viscosity of the fluid. Terminal velocity, or settling velocity, for a single spherical particle is shown in Equation 1 (Sahai and Moghanloo, 2019).

$$v_s = \frac{(\rho_p - \rho_f) g d^2}{18\mu} \tag{1}$$

Where v_s is particle settling velocity (m/s), ρ_p is density of the particle (kg/m^3), ρ_f is density of the transport fluid (kg/m^3), g is gravitational acceleration (m/s^2), d is particle diameter (m), and μ is viscosity of the transport fluid (Pa·s). Equation 1 can be rearranged to determine the maximum solid particle size that can travel to the surface of the outlet well without settling.

$$d_{max} = \sqrt{\frac{18\mu v_s}{(\rho_p - \rho_f) g}} \tag{2}$$

For Equation 2, it is assumed that the particle velocity is equal to the transport fluid velocity, $v_s = v_f$. This calculates the maximum particle size that reaches surface for a given fluid velocity. If $v_p > v_f$ it is expected that the particles would travel to surface. If $v_p < v_f$ it is expected that the particles would settle in the outlet well and therefore not reach the surface.

3.2 Assumptions and limitations of Stokes' Law

The analytical method of using Stokes' Law is formulated based on several assumptions (Ogolo et al., 2024):

- Particles are rigid, smooth, and spherical with a uniform density.
- The transport fluid is Newtonian and under laminar flow.
- There is no interaction between individual particles.
- Ignores wall/boundary effects.
- Temperature and viscosity of the transport fluid should be constant.
- Assuming a constant estimated solid particle density.

A main limitation to this analytical method is the assumption of laminar flow. Flow of the working fluid throughout the closed-loop geothermal system is expected to be transitional or turbulent based on the size of the system, higher fluid velocities, and low fluid viscosity at higher temperatures.

3.3 Comparative assessment

Stokes' Law was employed for comparative assessment against sample data. The sample used for this comparison is shown in Figure 3 and was collected during drilling activities involving loop circulation prior to start-up of the geothermal facility. Settling velocities were calculated for each measured particle size using Equation 1 and compared to the well fluid velocity, establishing the "cut-off" particle size expected to reach the surface. This assessment is shown in Figure 4.

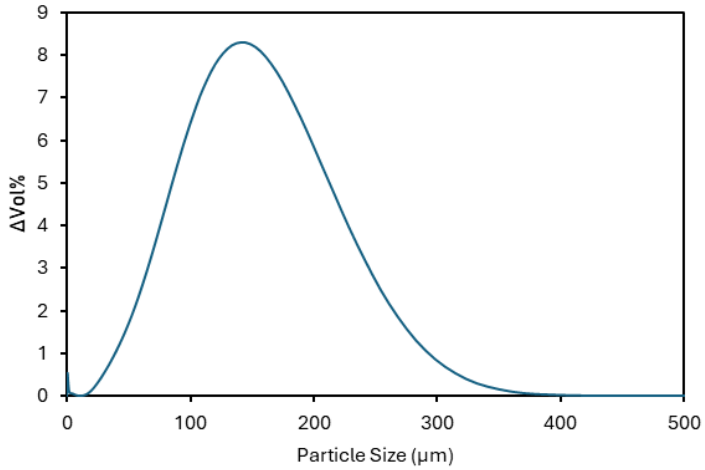


Figure 3. Particle size distribution for a sample collected at the outlet well at a circulation flow rate of 2.5 m^3/min.

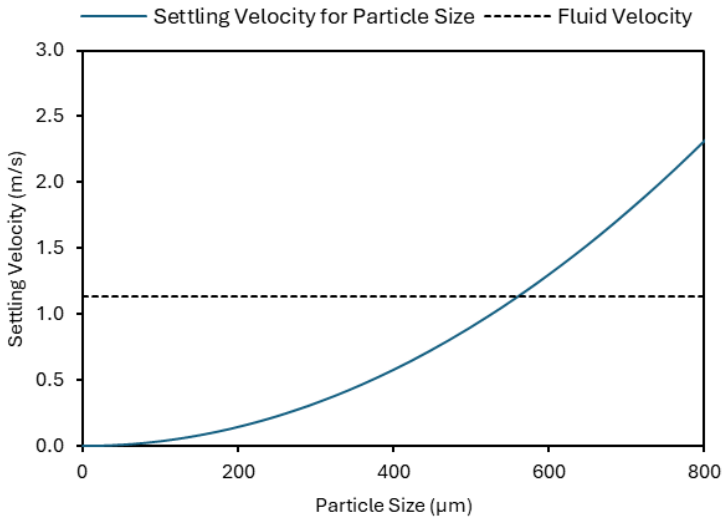


Figure 4. Calculated Stokes' Law settling velocity for each particle size measured from the sample shown in Figure 2 (blue). The settling velocities as a function of particle size are compared to the working fluid velocity (dashed line).

Figure 3 presents the particle size distribution (PSD) for the sample collected at the surface from the outlet well at a fluid velocity of approximately 1.1 m/s. Most particles were observed in the 50–300 μm range, with a mean diameter of 115 μm. Using Equation 1, the settling velocity for each particle size was calculated and plotted in Figure 4. The dashed horizontal line indicates the fluid velocity of 1.1 m/s, representing the threshold for particles expected to reach the surface. The intersection of the fluid velocity and settling velocity curves identifies a maximum transportable particle size of approximately 550 μm.

Stokes' Law establishes a deterministic settling velocity, providing a practical cut-off for the maximum particle size capable of remaining in suspension and producing a threshold-type deposition behavior. In contrast, measured PSDs as shown in Figure 3 follow a log-normal distribution, producing a gradual, probabilistic settling profile dependent on initial particle sizes. While Stokes' Law defines analytical limits, real systems exhibit continuous variation in particle sizes and stochastic settling behavior.

3.4 Schiller-Naumann correlation

To address the potential influence of moderate turbulence and elevated Reynolds numbers under variable flow conditions in the closed-loop system, a drag-based correlation was integrated into the Stokes' Law framework. The Schiller–Naumann correlation provides an empirical relationship for the drag coefficient applicable to transitional and moderately turbulent flow regimes for Newtonian fluids (Yan et al., 2021). The drag coefficient, C_D, represents the ratio of viscous resistance to inertial forces acting on a particle during settling and depends on both particle and fluid properties. For spherical particles in a Newtonian fluid, the particle Reynolds number is expressed in Equation 3 below.

$$Re = \frac{\rho_f v_s d_p}{\mu} \tag{3}$$

Where ρ_f is density of the transport fluid (kg/m^3), v_s is particle settling velocity (m/s), d_p is particle diameter (m), and μ is viscosity of the transport fluid (Pa·s). The correlation for Schiller-Naumann is shown in Equation 4 (Xu et al., 2024).

$$C_D = \frac{24}{Re}(1 + 0.15Re^{0.687}) \tag{4}$$

Where Re is the Reynolds number calculated using Equation 3.

Terminal settling velocity, incorporating the drag correction, was determined from the modified Stokes' Law expression (Walsh and Rao, 1988) as shown in Equation 5.

$$v_s = \sqrt{\frac{4(\rho_p - \rho_f)gd}{3C_D\rho_f}} \tag{5}$$

Where v_s is particle settling velocity (m/s), ρ_p is density of the particle (kg/m^3), ρ_f is density of the transport fluid (kg/m^3), g is gravitational acceleration (m/s^2), d is particle diameter (m), and C_D is the drag coefficient calculated using Equation 4.

A comparative assessment was performed for the sample data presented previously in Figure 3. Results from Stokes' Law in Figure 4 are included for reference.

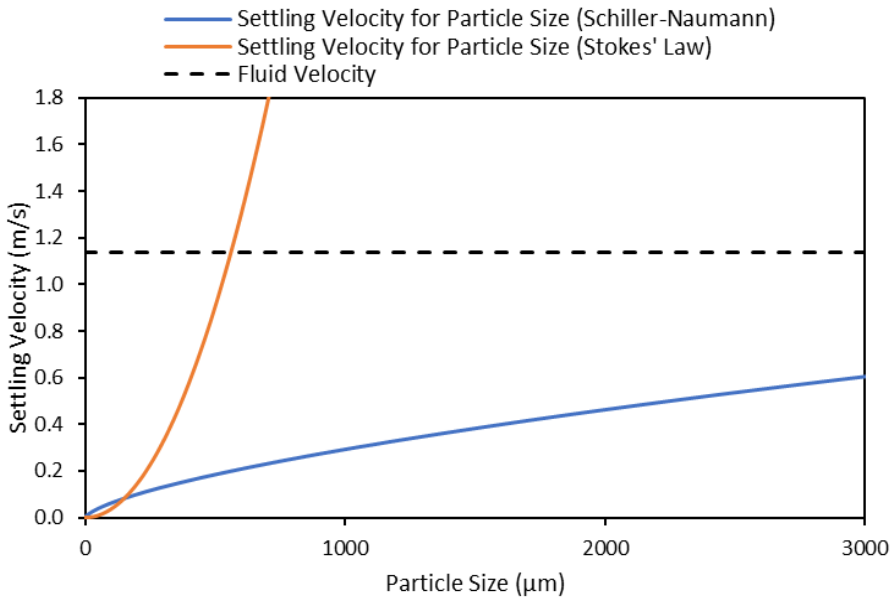


Figure 5. Calculated Schiller-Naumann correlation settling velocity for each particle size measured from the sample shown in Figure 3 (blue). The settling velocities as a function of particle size are compared to

the working fluid velocity (dashed line). Settling velocities using Stokes' Law are shown for reference (orange).

Settling velocities for each particle size were calculated using Equation 5 and plotted in Figure 5. The dashed horizontal line at 1.1 m/s represents the fluid transport velocity, defining the threshold for particles expected to reach the surface. The intersection of the fluid velocity and the calculated settling velocity curve identifies the maximum transportable particle size. Relative to the Stokes' Law model assuming laminar flow, incorporation of the Schiller–Naumann drag correction predicts greater particle mobility, with larger particles remaining entrained in the flow and being transported to surface. This adjustment provides a more realistic representation of particle settling under transitional or minimally turbulent conditions.

The Schiller-Naumann correction accounts for higher Reynolds numbers, reducing drag and predicting larger particles reaching the surface. However, sample data shown in Figure 5 indicates the model overestimates the maximum particle size observed, suggesting the flow transports larger particles less effectively than predicted. The smaller particle sizes shown in Figure 3 may result from particle aggregation or flocculation, or a smaller particle size distribution at the bottom of the outlet well which cannot be predicted with certainty.

4 EMPIRICAL PROBABLISTIC MODEL

An empirical probabilistic model was implemented as an alternative to analytical models using Stokes' Law and Schiller-Naumann to better capture the particle settling behaviour observed at the surface of the closed-loop system. A hybrid physics-based numerical framework was developed to predict the transport and surface accumulation of particles, assuming a log-normal distribution of particle sizes within the outlet well.

As shown previously in Figure 3, the particle size distribution (PSD) of solids in the geothermal working fluid exhibits a log-normal distribution. Based on this observation, it is assumed that two distinct PSDs are relevant for predictive modelling of particle settling: the bottomhole PSD and the surface PSD. The discrepancy between these distributions can be attributed to a size-dependent survival probability of particle settling during transport, influenced by stochastic turbulent fluctuations in the flow.

The predictive model chosen is a probabilistic settling model that can forecast surface particle size distributions under variable flow rate conditions. The model can also be inverted to predict bottomhole particle size distributions based on data obtained from samples at surface. This statistical model provides a survival analysis where the functions $f(t)$, $F(t)$, and $S(t)$ mathematically predict distributions of a lifetime variable, T.

$$f(t) = h(t) \times S(t) \tag{6}$$

Where $f(t)$ denotes the probability density function (PDF), $h(t)$ is the approximate probability, also known as the hazard function, and $S(t)$ is known as the reliability function (Lawless, 2003). Based on Equation 6, the relationship between the bottomhole PSD, $f_b(d)$, and the surface PSD, $f_s(d)$, can then be expressed as shown in Equation 7.

$$f_s(d) = f_b(d) \times P_{survival}(d) \tag{7}$$

Where $P_{survival}(d) \in [0,1]$ is a survival function that represents the probability of a particle of diameter d being lifted from the bottom of the well to the surface of the well. The survival probability is influenced by turbulent forces, which can be modeled as a stochastic process. This formulation enables predictive modelling of the surface PSD based on the bottomhole PSD and the dynamics of particle transport under turbulent conditions.

4.1 Parametric survival probability function

To determine the survival function, $P_{survival}$, the Weibull parametric survival model can be applied. Specifically, the two-parameter generalized exponential distribution can be used effectively as it contains a right skewed hazard function. The Weibull distribution model has two dimensionless empirical parameters λ and m for scale and shape, respectively. The cumulative hazard function is $\Lambda(d) = \lambda(h(d))^m$ and represents the total accumulated risk of an event occurring for variable d. For a two-parameter Weibull distribution, the survival function is then shown in Equation 8.

$$P_{survival}(d) = \exp\{-\lambda(h(d))^m\} \tag{8}$$

Where λ and m are the function parameters, h represents the hazard function, d is particle diameter, and $d > 0$ for $\lambda, m > 0$ (Kalbfleisch and Prentice, 2002).

With various combinations of λ and m as fit parameters, the Weibull distribution is flexible at representing various probability processes. The parameter λ is a scale factor that represents the characteristic particle size. An increase in λ shifts the particle size distribution towards larger particle diameters, whereas a decrease in λ shifts the particle size distribution towards smaller particle diameters. The parameter m is a shape factor that determines the failure rate. For $m < 1$ the hazard rate is decreasing, for $m = 1$ the hazard rate is constant, and for $m > 1$ the hazard rate is increasing. A plot of the of the two parameter Weibull distribution is presented in Figure 6 below for context.

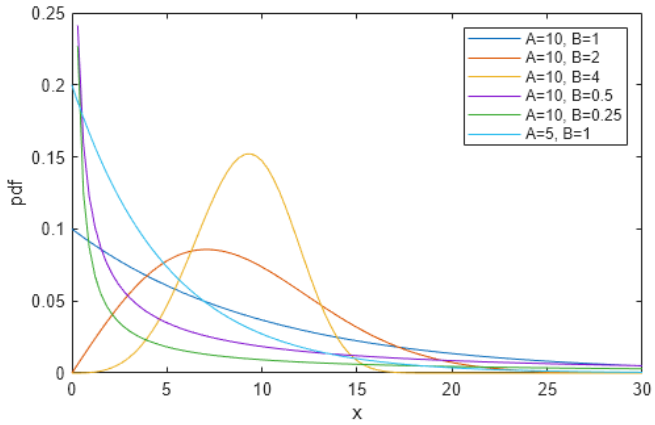


Figure 6. Weibull distributions with various combinations of λ and m (MathWorks, 2025).

4.2 Physics based modelling

For particle settling analysis employing the Weibull distribution survival function, $h(d)$ can be substituted with physics-based formulations to represent the particle settling velocity as a function of local turbulence. In this context, the survival function characterizes the probability that a particle of a given size reaches the surface of the outlet well. In the physics-based framework, the survival probability is predicted based on the particle settling velocity normalized by a measure of turbulence intensity:

$$h(d) = \frac{v_s(d)}{\sigma_u} \tag{9}$$

Where v_s denotes the settling velocity for a given particle size, d, and σ_u represents a turbulence intensity proxy. The settling velocity, v_s, can be calculated based on an appropriate flow regime, with common models including Stokes' Law or the Schiller-Naumann correlation. The turbulence intensity proxy is estimated for fully developed pipe flow and shown as the following equation:

$$\sigma_u = IU \tag{10}$$

Where $I \sim 0.16\, Re^{-1/8}$ represents the turbulence intensity (ANSYS, 2022), and $U = 4Q/(\pi D^2)$ corresponds to the bulk velocity of the transport fluid. For the bulk velocity, Q is the volume flow rate (m^3/s) and D is the pipe diameter (m).

The survival function also becomes a function of length, L, since the probability of survival decreases with both the distance travelled through the outlet well and the transit time. To account for this dependency, the local hazard per unit length is scaled by the dimensionless ratio, L/D. Here, L is the particle travel distance and D is the characteristic pipe diameter. The updated survival function is expressed as Equation 11 below.

$$P_{survival}(d|L) = \exp\left\{-\lambda \left(\frac{v_s(d)}{\sigma_u}\right)^m \frac{L}{D}\right\} \tag{11}$$

Where λ is the dimensionless hazard coefficient, $v_s(d)$ is the particle settling velocity (m/s), σ_u is the turbulence intensity, m is a dimensionless model exponent, L is the length of the outlet well (m), and D is the diameter of the outlet well (m).

4.3 Bottomhole PSD uncertainty

A primary limitation of the current model is the accurate quantification of the bottomhole particle size distribution (PSD), $f_b(d)$. Direct prediction of the bottomhole PSD is not feasible for the probabilistic model without further experimentation. To address this constraint, two laboratory-measured surface PSD datasets

were modified using scaling and mixing parameters to generate a representative bottomhole PSD. This method produces a physically realistic bottomhole distribution and eliminates circular dependencies within the probabilistic framework to avoid deriving the bottomhole PSD from the same surface PSD data used for model calibration and prediction.

4.4 Parameter fitting and model calibration

When only a single surface PSD is available, the bottomhole PSD is inferred using the measured surface PSD and initial estimates of the dimensionless parameters λ and m, defining the source distribution. With at least two surface PSDs under varying flow conditions, λ and m are optimized by minimizing the error between one of the predicted and observed surface PSDs. This ensures the survival function accurately represents particle transport in the system. The calibrated model can then be applied in a forward simulation to predict surface PSDs at new flow rates, allowing for quantitative forecasting of particle size settling under varying conditions.

4.5 Results

Preliminary results from the probabilistic model match and prediction are presented in Figure 7**Fehler! Verweisquelle konnte nicht gefunden werden.**. The model was initialized using a fixed inlet PSD described in Section 4.44.4, and global parameter values were then fitted to best represent the system behavior for a sample collected during loop circulation prior to startup at 2.5 m^3/min. A predicted PSD is then plotted for a flow rate of 2 m^3/min. For this model, particle settling velocities incorporated into the survival probability function shown in Equation 11 were calculated according to Schiller-Naumann.

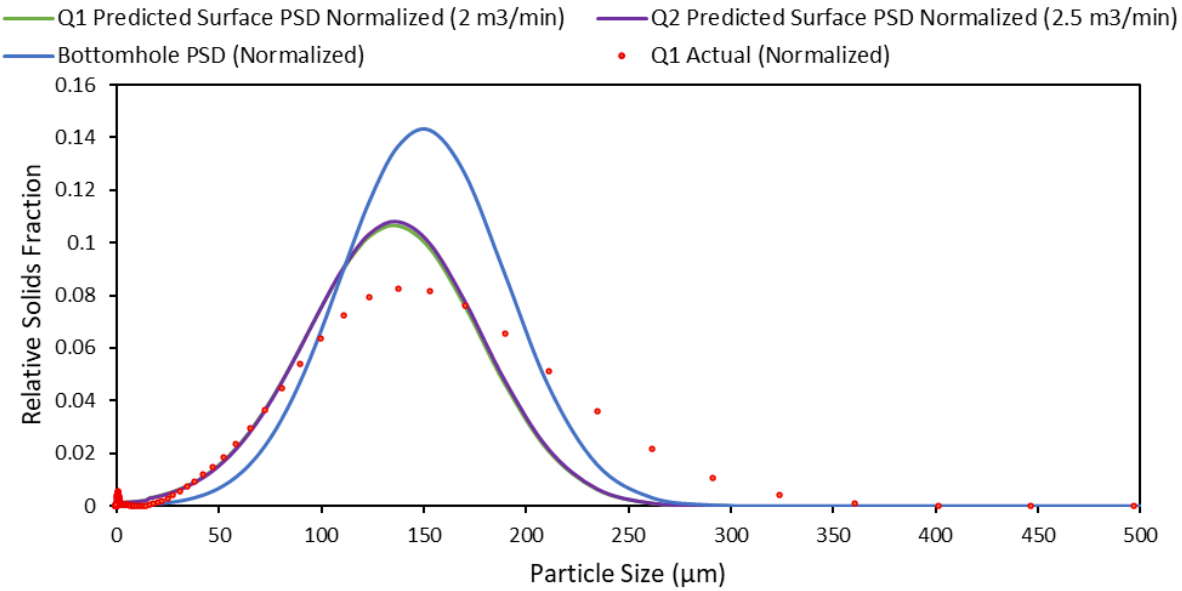


Figure 7. Normalized results from the probabilistic model comparing the bottomhole PSD with surface PSDs at a loop circulation rate of 2.5 m^3/min, Q1, and 2 m^3/min, Q2.

From Figure 7**Fehler! Verweisquelle konnte nicht gefunden werden.**, it is evident that the predicted surface PSDs show a slightly smaller mean particle size. This is consistent with expectations, as larger particles are more likely to settle due to physics-based parameters in the model. The match in this instance follows the same trend as the experimental data, though testing against a larger sample of possible bottomhole PSDs should improve the match.

A key observation from this modelling is that the difference between 2 m^3/min and 2.5 m^3/min on the predicted particle size distributions is quite small, meaning a larger difference in flow rates is likely required to provide meaningful predicting power. At the time of writing, more experimental data was not available to test the model, however, future work is expected to confirm validity.

5 FURTHER INVESTIGATION

The modelling conducted in this study provides the probability of particles of a particular size reaching the surface under a given flow condition. Future work will involve increasing the frequency of sampling during operations to test the models' predictions against actuals. Another area of future work is developing a time-

domain model of particle settling within the system, with the goal of not only modelling which particles will make it to surface, but also when the particles will reach the surface. This approach aims to capture transient settling dynamics, offering a more comprehensive understanding of particle behaviour over time. Combining the time-based transport dynamics with probabilistic modelling and simulations will also allow us to learn more about the bottomhole PSD by tracking the distribution of generated particles up the wellbore.

Further experimentation for reducing bottomhole PSD uncertainty is also required. A potential experimental setup could involve circulating an initial PSD through a standpipe at controlled flow rates, followed by quantitative measurement of the resulting surface PSD. This approach serves as a laboratory-scale simulation of the geothermal system, allowing for the assessment of particle transport and deposition behavior under varying hydraulic conditions. Additional analysis of the solid samples is also required to determine the densities of particles reaching surface. This will allow measured values to be used in place of a uniform density assumption.

Consideration of additional mechanisms influencing particle settling can be incorporated in future modelling. A key factor influencing particle settling is inter-particle interactions, including aggregation and flocculation, which can be represented using population balance equations to capture the time-dependent evolution of particle size distributions (Shi et al., 2019). Such interactions contribute to hindered settling. Furthermore, environmental boundary effects can influence particle settling. Wall-induced obstruction of settling can be quantified as a function of the Reynolds number and the ratio of particle to wall geometry dimensions (Arsenijevic et al., 2010). Another impactful consideration for future work is incorporation of the drag coefficient as it relates to spherical and nonspherical particles.

6 CONCLUSION

Findings from this study indicate that solid particles in the geothermal working fluid exhibit behavior consistent with a log-normal size distribution. To assess the probability of particles of varying sizes reaching the surface of a geothermal well, physics-based probabilistic modelling offers a more robust approach than conventional analytical threshold models, such as Stokes' Law. The accuracy of probabilistic models can be further enhanced through extensive operational data collection and targeted experimentation that allows for more accurate prediction of bottomhole particle size distributions. By providing a quantitative framework for particle transport and settling in geothermal wells, this study demonstrates how predictive assessment of solid settling can guide mitigation strategies to reduce operational risks to geothermal surface facilities.

Acknowledgements

The authors acknowledge and thank Hydroisotop GmbH for providing laboratory testing and particle size distribution data for this study. Appreciation is also extended to the Eavor Geretsried project site team for access to sampling and their additional technical support.

REFERENCES

ANSYS, Inc.: ANSYS Fluent User's Guide, Release R1, Canonsburg, PA, United States of America (2022).

Arsenijevic, Z.L., et al.: Wall effects on the velocities of a single sphere settling in a stagnant and counter-current fluid and rising in a co-current fluid, Powder Technology, 203, (2019), 237-242.

Kalbfleisch, J.D., and Prentice, R.L.: The Statistical Analysis of Failure Time Data, Wiley-Interscience, Hoboken, New Jersey, United States of America (2002).

Lawless, J.F.: Statistical Models and Methods for Lifetime Data, Wiley-Interscience, Hoboken, New Jersey, United States of America (2003).

MathWorks (The MathWorks, Inc.): Weibull Distribution - MATLAB & Simulink Help, "Weibull Distribution," MathWorks Documentation (2025).

Ogolo, N.A., et al.: Problems of Stokes' law application in determining the settling velocity of clays, Journal of Engineering Sciences and Innovation, 9, (2024), 277-286.

Sahai, R., and Moghanloo, R.G.: Proppant transport in complex fracture networks - A review, Journal of Petroleum Science and Engineering, 182, (2019), 3-4.

Shi, Z., et al.: Modeling of Flocculation and Sedimentation Using Population Balance Equation, Journal of Chemistry, (2019).

Walsh, D.E., and Rao, P.D.: A Study of Factors Suspected of Influencing the Settling Velocity of Fine Gold Particles, University of Alaska Fairbanks, Fairbanks, Alaska, United States of America (1988).

White, M., et al.: Numerical investigation of closed-loop geothermal systems in deep geothermal reservoirs, Geothermics, 116, (2024), 1-2.

Xu, Z., et al.: A New Model for Predicting Drag Coefficient and Settling Velocity of Coarse Mineral Particles in Newtonian Fluid, Minerals, 14(2), (2024), 150.

Yan, T., et al.: A novel predictive model of drag coefficient and settling velocity of drill cuttings in non-Newtonian drilling fluids, Petroleum Science, 18, (2021), 1729-1738.